SCIENCE CHINA
Life Sciences

SPECIAL TOPIC: Calcium signaling
• RESEARCH PAPER•

August 2016 Vol.59 No.8: 811–824
doi: 10.1007/s11427-016-5094-6

Expression and reconstitution of the bioluminescent Ca^{2+} reporter aequorin in human embryonic stem cells, and exploration of the presence of functional IP_3 and ryanodine receptors during the early stages of their differentiation into cardiomyocytes

Harvey Y.S. Chan[1], Man Chun Cheung[2], Yi Gao[2], Andrew L. Miller[1,3] & Sarah E. Webb[1*]

[1]*Division of Life Science & State Key Laboratory of Molecular Neuroscience, HKUST, Clear Water Bay, Hong Kong, China;*
[2]*Stem Cell & Regenerative Medicine Consortium, Li Ka Shing Faculty of Medicine, The University of Hong Kong, Pokfulam, Hong Kong, China;*
[3]*Marine Biological Laboratory, Woods Hole MA 02543, USA*

Received March 23, 2015; accepted May 6, 2016; published online July 15, 2016

In order to develop a novel method of visualizing possible Ca^{2+} signaling during the early differentiation of hESCs into cardiomyocytes and avoid some of the inherent problems associated with using fluorescent reporters, we expressed the bioluminescent Ca^{2+} reporter, apo-aequorin, in HES2 cells and then reconstituted active holo-aequorin by incubation with *f*-coelenterazine. The temporal nature of the Ca^{2+} signals generated by the holo-*f*-aequorin-expressing HES2 cells during the earliest stages of differentiation into cardiomyocytes was then investigated. Our data show that no endogenous Ca^{2+} transients (generated by release from intracellular stores) were detected in 1–12-day-old cardiospheres but transients were generated in cardiospheres following stimulation with KCl or $CaCl_2$, indicating that holo-*f*-aequorin was functional in these cells. Furthermore, following the addition of exogenous ATP, an inositol trisphosphate receptor (IP_3R) agonist, small Ca^{2+} transients were generated from day 1 onward. That ATP was inducing Ca^{2+} release from functional IP_3Rs was demonstrated by treatment with 2-APB, a known IP_3R antagonist. In contrast, following treatment with caffeine, a ryanodine receptor (RyR) agonist, a minimal Ca^{2+} response was observed at day 8 of differentiation only. Thus, our data indicate that unlike RyRs, IP_3Rs are present and continually functional at these early stages of cardiomyocyte differentiation.

Ca^{2+} signaling, apo-aequorin expression, bioluminescence, HES2 human embryonic stem cells, hESC-derived cardiospheres, IP_3 and ryanodine receptors

Citation: Chan, H.Y.S., Cheung, M.C., Gao, Y., Miller, A.L., and Webb, S.E. (2016). Expression and reconstitution of the bioluminescent Ca^{2+} reporter aequorin in human embryonic stem cells, and exploration of the presence of functional IP_3 and ryanodine receptors during the early stages of their differentiation into cardiomyocytes. Sci China Life Sci 59, 811−824. doi: 10.1007/s11427-016-5094-6

INTRODUCTION

It has long been known that Ca^{2+} signaling plays a key role in many aspects of embryonic development (Jaffe, 1999; Berridge et al., 2000; Webb and Miller, 2003; Whitaker, 2006, Webb et al., 2011; Rosenberg and Spitzer, 2011), as well as controlling a wide variety of cellular functions (Szent-Györgyi, 1975; Berridge, 1993; Peterson et al., 1994; Bootman and Lipp, 2001; West et al., 2001). Indeed, well-defined Ca^{2+} signals have been demonstrated to correlate with, and sometimes to directly initiate and/or regulate, distinct morphological events (Homa et al., 1993; Swann et al., 1994; Chang and Meng, 1995; Webb et al., 1997; Leung et al., 1998; Créton et al., 2000; Porter et al., 2003; Ma et

*Corresponding author (email: barnie@ust.hk)

al., 2009; Lohmann, 2009; Cheung et al., 2011). In addition, when errors occur in the normal pattern of Ca^{2+} signaling, these might result in the onset of a particular disorder or disease (Somlo and Erlich, 2001; Splawski et al., 2004; Allen et al., 2010; Woods and Padmanabhan, 2012).

The essential role of Ca^{2+} in the contraction of the mature heart was first identified over a century ago (Ringer, 1883). This process, called "excitation-contraction" coupling, is now known to be a highly complex mechanism involving a number of tightly-coupled ion channels and transporters that regulate Ca^{2+} entry from (and exit to) the extracellular environment as well as Ca^{2+} release from (and uptake into) intracellular stores such as the sarcoplasmic reticulum (SR). This highly regulated process has long been known to involve L-type Ca^{2+} channels and the Na^{+}/Ca^{2+} exchanger (NCX) in the plasma membrane, and ryanodine receptors (RyRs) and the sarco/endoplasmic reticulum Ca^{2+} ATPase (SERCA) in the SR (reviewed by Bers, 2002; Seidler et al., 2007; Zhao et al., 2015). More recently, Ca^{2+} release via inositol 1,4,5-trisphosphate receptors (IP_3Rs) in the SR, and via the two pore channel 2 (TPC2) in lysosomes, Ca^{2+} extrusion via the plasma membrane Ca^{2+} ATPase (PMCA), Ca^{2+} uptake into and release from mitochondria via a Ca^{2+} uniporter and mitochondrial NCX, and modulation of Ca^{2+} via sympathetic activation have been identified to play a role in normal heart function (Bers, 2002; Hund et al., 2008; Griffiths, 2009; Mohamed et al., 2010; Capel et al., 2015; Nita et al., 2015). Thus, we now know that the precise level of Ca^{2+} is maintained via the complex interaction between a range of different Ca^{2+} channels and receptors located in various organelles as well as in the plasma membrane. If this tight control of the intracellular Ca^{2+} concentration is lost then the cells undergo necrosis or apoptosis, which can lead to myocardial infarction and heart failure (Schaper et al., 1999; Gill et al., 2002; Lim et al., 2007; Konstantinidis et al., 2012; Fischer et al., 2013).

As well as regulating mature heart function via excitation-contraction coupling (Bers, 2002; Seidler et al., 2007; Greenstein and Winslow, 2011), Ca^{2+} signaling has also been shown to play a role in heart development (Pucéat and Jaconi, 2005), via various different pathways and mechanisms, termed "excitation-transcription" coupling (Wu et al., 2006; Seidler et al., 2007). In zebrafish embryos, for example, a series of Ca^{2+} transients were observed to be generated in the region of the developing heart; these transients were generated every 10–20 min and the Ca^{2+} concentration was elevated 10-fold higher than the normal background level of Ca^{2+} (Créton et al., 1998). In addition, when embryos were treated with a Ca^{2+} buffer, BAPTA, one of the most obvious effects was the development of a defective heart; even though a distinct atrium and ventricle were still formed, the heart was smaller than normal and was not capable of pumping blood (Créton et al., 1998). In the chick, when embryos were treated with ouabain or ionomycin to increase the intracellular Ca^{2+} either indirectly (via the NCX) or directly, respectively, differentiation of the cells in the posterior areas of the heart-forming region was blocked (Linask et al., 2001). In addition, treatment with KB-R7943, an NCX inhibitor, affected the early development of the heart and blocked the initial heart beats in the chick embryo (Linask et al., 2001). Ca^{2+} signaling also plays a key role in heart development in mammals. For example, when mouse embryos were cultured with nifedipine or verapamil (both L-type Ca^{2+} channel blockers), they developed hearts with an enlarged left ventricle, no right ventricle, a longer and thinner than normal outflow tract and abnormal cardiac looping (Porter et al., 2003). Nifedipine treatment also affected the expression of some but not all the cardiac genes, thus supporting the excitation-transcription model.

In addition to the research conducted with intact animal models, many more reports describe the role of Ca^{2+} signaling in developing and differentiating cardiomyocytes cultured *in vitro* (Sauer et al., 2001; Dolnikov et al., 2005; Janowski et al., 2006; Fu et al., 2006; Liu et al., 2007, and reviewed in Bers, 2008, Lee and Siu, 2012). One point that has become eminently clear, however, is that there is a high level of diversity in the characteristics of the Ca^{2+} signals generated and thus the relative roles of the varying elements of the Ca^{2+} signaling toolbox, when comparing cardiomyocytes isolated from different species (Liu et al., 2002; Galli et al., 2006; Janowski et al., 2006; Zhang et al., 2011). Thus, although studies with animals have generated a lot of useful information regarding the development of the heart and the role of Ca^{2+} signaling in this process, there is still a lot to discover about the development and regeneration of the human heart with respect to this essential second messenger. Research on human cardiomyocytes has progressed rapidly in recent years following the development of methods to generate cardiomyocytes from embryonic stem cells (ESCs) and induced pluripotent stem cells (iPSCs) with the long-term strategy being that these cells might be applied in a clinical setting to treat heart disease (Krane et al., 2010; Kong et al., 2010; Poon et al., 2011).

In the majority of studies conducted so far to investigate the Ca^{2+} handling properties of human stem cells or cardiomyocytes derived from stem cells, intracellular Ca^{2+} signals have been visualized using various fluorescent Ca^{2+} indicators. In the case of reporters such as Fluo-3 (Lee et al., 2011), Fluo-4 (Satin et al., 2008; Apáti et al., 2013), and Fura-2 (Dolnikov et al., 2006; Liu et al., 2007), cells were loaded with the dye via incubation with the respective acetoxymethyl (AM) ester. However, the problems of using such dyes for measuring Ca^{2+} signals inside cells with regards to the uneven distribution of the dye both within single cells via reporter compartmentalization and in beating clusters of cells, have been emphasized for both hESCs and hESC-CMs (Apáti et al., 2012, 2013). Most recently, the development of stem cell-derived cardiomyocytes that stably express genetically encoded fluorescent Ca^{2+} reporters

based on GCaMP has been described. These include the stable expression of: GCaMP3 in H7 hESCs (Shiba et al., 2012); GCaMP2 in HUES9 hESCs (Apáti et al., 2013); and GCaMP6f in induced-pluripotent stem cells (Maddah et al., 2015). Being genetically expressed, these fluorescent reporters do not have the loading issues of some of the fluorescent dyes such as Fluo-4 (Apáti et al., 2013). In addition, at least one of the GCaMP variants has been demonstrated to be able to detect Ca^{2+} transients in long-term imaging experiments that were conducted over several months (Tian et al., 2009). However, genetically encoded fluorescent Ca^{2+} reporters do have some drawbacks when compared with synthetic reporters with regards to their signal-to-noise ratio and photostability. Regarding the latter, the protein stability of GCaMP reporters has been reported to be low (Tian et al., 2009).

Bioluminescent Ca^{2+} reporters such as aequorin provide an alternative means of measuring Ca^{2+} inside cells, either in the cytosol or within specific compartments via targeting (Rizzuto et al., 1992). Indeed, bioluminescent Ca^{2+} reporters have a number of advantages over fluorescent Ca^{2+} reporters. For example, in the presence of Ca^{2+}, light is generated without the need for excitation and so the autofluorescence, photobleaching and photo-toxicity that can be problematic with fluorescent reporters (especially during long-term imaging) are not an issue with bioluminescent reporters (Miller et al., 1994). In addition, aequorin has, over the years, been shown to be non-disturbing and therefore it does not affect the normal development of embryos or the function of cells (Miller et al., 1994; Silver, 1996). It is suggested, therefore, that likewise, it will not affect the normal proliferation and differentiation of ESCs. Finally, aequorin has a wide dynamic range such that it can be used to measure changes in free cytosolic Ca^{2+} between 0.1 to 100 μmol L^{-1}, and it exhibits a high level of inherent contrast enhancement such that the level of luminescence generated is approximately proportional to the square of the free [Ca^{2+}] (Shimomura and Inouye, 1996). Together, these various characteristics of bioluminescent Ca^{2+} reporters such as aequorin allow the ready detection and/or visualization of even the smallest changes in intracellular [Ca^{2+}] continually over the relatively long time periods that are required to monitor ESC differentiation. Aequorin has long been the method of choice for recording Ca^{2+} signals in large cells such as muscle fibers and axons (Ridgway and Ashley, 1967; Baker et al., 1971), and in eggs and early embryos of fish, frogs and sea urchins (Ridgway et al., 1977; Eisen and Reynolds, 1985; Webb et al., 1997; Leclerc et al., 2000), which can be loaded with the reporter via microinjection. However, the protein component of aequorin (i.e., apo-aequorin) can also be genetically introduced into cells, after which active holo-aequorin is reconstituted *in vivo* by simple incubation with its prosthetic co-factor, coelenterazine (Rizzuto et al., 1992). The first demonstration of apo-aequorin being genetically expressed in cells was reported in the early 1990s when the Tex-mex tobacco plant (*Nicotiana plumbaginifolia*) was successfully transformed with the protein (Knight et al., 1991). This group went on to show that when aequorin was reconstituted in whole plants via incubation with coelenterazine, then they could measure changes in Ca^{2+} in response to wind, touch, cold-shock, fungal elicitors, and wounding (Knight et al., 1991, 1992, 1993). Since then, apo-aequorin has been genetically expressed in a variety of animal and plant species, as well as in cells in culture (reviewed in Webb et al., 2010). However, whereas apo-aequorin has previously been genetically expressed in cardiomyocytes isolated from adult rats (Bell et al., 2006), it has not been expressed in human stem cell-derived cardiomyocytes before now.

In this new study, the HES2 human embryonic stem cell line was transduced with apo-aequorin. These cells were then used to investigate the onset of functionality of the two main SR-localized Ca^{2+} channels (i.e., IP_3R and RyR) during the earliest stages of cardiomyocyte differentiation. Thus, cardiospheres at day 1, 4, 8 and 12 of differentiation were incubated with *f*-coelenterazine to reconstitute active holo-*f*-aequorin (also called *f*-aequorin). The result of applying ATP or caffeine on the generation of Ca^{2+} signals was then recorded using a luminometer in order to assess whether (and if so, then when), IP_3Rs and RyRs, respectively, were functional in these cells.

RESULTS

Transduction of HES2 cells with the pLV-EF1α-tdTomato-T2A-Apoaequorin (ETO-AEQ) plasmid

Figure 1 demonstrates that HES2 cells were successfully transduced with the apo-aequorin gene. Figure 1A shows a representative image of a cluster of HES2 cells expressing tdTomato, and Figure 1B is a Western blot showing the expression of apo-aequorin in cells at passages 57 and 59.

Measuring endogenous Ca^{2+} signals in holo-*f*-aequorin-expressing cardiospheres

An investigation was conducted to determine if any endogenous Ca^{2+} signals could be detected in the holo-*f*-aequorin expressing cells via release from the major intracellular Ca^{2+} store in heart muscle cells, i.e., the SR (Figure 3A). Thus, cardiospheres at day 8 of differentiation (Figure 2A) were incubated in essentially Ca^{2+}-free bathing medium (i.e., Ca^{2+}-free phosphate buffer saline (PBS) with 5 μmol L^{-1} EGTA) for 160 min. Our data showed that the luminescence intensity remained at a basal level of ~580 counts per second (cps) for the duration of the Ca^{2+} measurements and no intracellular Ca^{2+} transients were detected over this time period. At the end of the experiment, 5% Triton X-100

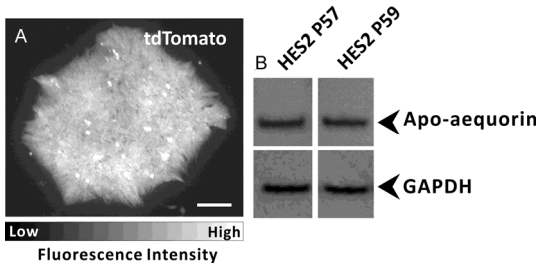

Figure 1 HES2 cells that had been transduced with the pLV-EF1α-tdTomato-T2A-Apoaequorin (ETO-AEQ) lentivirus express both A) tdTomato and B) apo-aequorin. A, Expression of tdTomato in a cluster of HES2 cells. Scale bar, 20 μm. B, Western blot to show the expression of apo-aequorin at two passages of HES2 cells (i.e., P57 and P59). GAPDH was used as a loading and membrane transfer control.

(Figure 2B) was added to the sample to lyse the cardiospheres and thus burn-out any remaining unspent holo-*f*-aequorin, and this stimulated a ~27-fold increase in luminescence intensity (from ~580 cps to ~16,163 cps; Figure 2B). Thus, even though no endogenous Ca^{2+} signals were recorded from the cardiospheres, there appeared to be sufficient active holo-*f*-aequorin in the cells to generate a signal if an endogenous Ca^{2+} event occurred.

KCl and $CaCl_2$ stimulate the generation of Ca^{2+} signals in apo-aequorin-expressing cardiospheres

Figure 2C and D shows two representative line graphs demonstrating the effect of 20 mmol L^{-1} KCl and 1 mmol L^{-1} $CaCl_2$ on the holo-*f*-aequorin-generated bioluminescence in cardiospheres at day 8 (Figure 2C) and day 18 (Figure 2D). In the day 8 cardiospheres (Figure 2C), the luminescence intensity increased rapidly by ~0.4-fold (i.e., from ~966 cps to ~1,393 cps and from ~852 to ~1,190 cps) following each addition of KCl. Three subsequent additions of $CaCl_2$ stimulated the luminescence intensity to increase by ~0.3 to 0.5-fold (i.e., from ~740 to ~1,093 cps, from ~596 to ~912 cps, and from ~584 to ~785 cps, respectively). During the ~30 min of the luminescence measurements, the background level of luminescence also decreased from ~1,000 to ~525 cps.

The day 18 cardiospheres (Figure 2D) exhibited a more robust response to treatment with both KCl and $CaCl_2$. For example, on addition of KCl, the luminescence intensity increased by ~1.5-fold (i.e., from ~514 to ~1,273 cps) before decreasing back to a background level of ~523 cps. The two subsequent additions of $CaCl_2$ both resulted in the

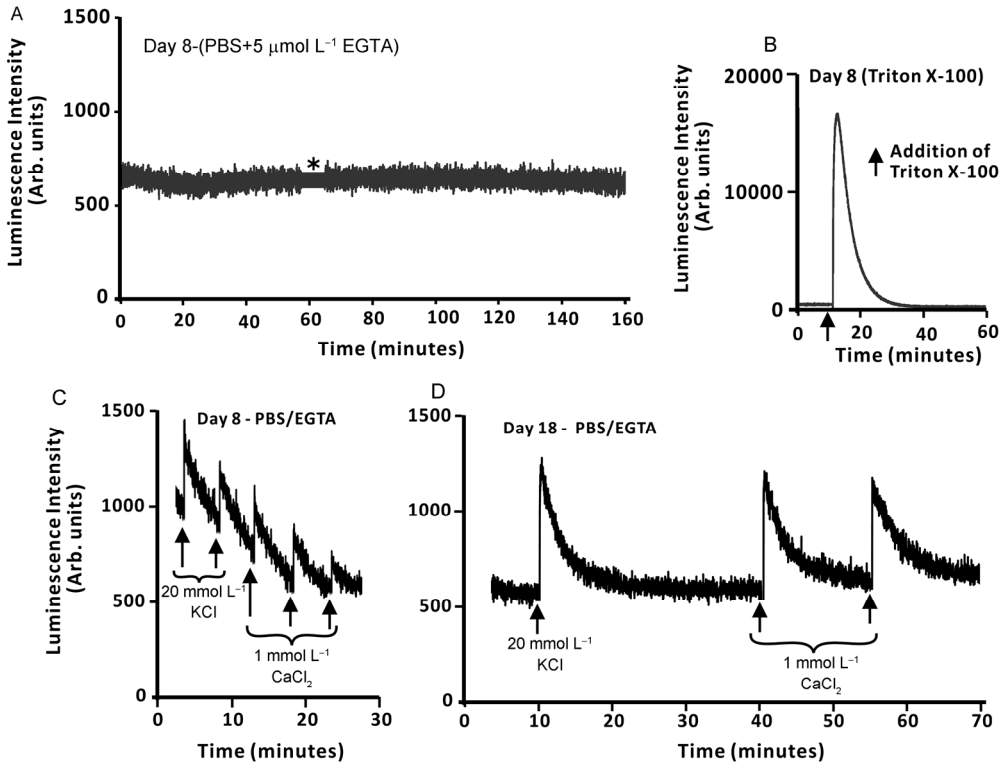

Figure 2 Representative line graphs to confirm the functionality of holo-*f*-aequorin in the HES2-derived cardiomyocytes. A, No endogenous Ca^{2+} signals were generated in cardiospheres at day 8 of differentiation. Cardiospheres were incubated with *f*-coelenterazine for 45 min, after which they were washed briefly with PBS and then incubated with PBS containing EGTA for the course of the luminescence intensity measurements. The asterisk indicates a brief break (of ~7 min) in the luminescence intensity recording. B, At the end of the Ca^{2+} measurements, 5% Triton X-100 (black arrow) was added to the cardiosphere sample in order to lyse the cells and burn-out any remaining unspent aequorin. C and D, The effect of KCl and $CaCl_2$ on the aequorin-generated luminescence in cardiospheres at (C) day 8 and (D) day 18 of differentiation. Cardiospheres were incubated with *f*-coelenterazine for 45 min, after which they were washed briefly with PBS and then incubated with PBS containing EGTA for the course of the luminescence intensity measurements. KCl (at 20 mmol L^{-1}) and $CaCl_2$ (at 1 mmol L^{-1}) were applied to the cardiosphere samples at the times indicated (see black arrows).

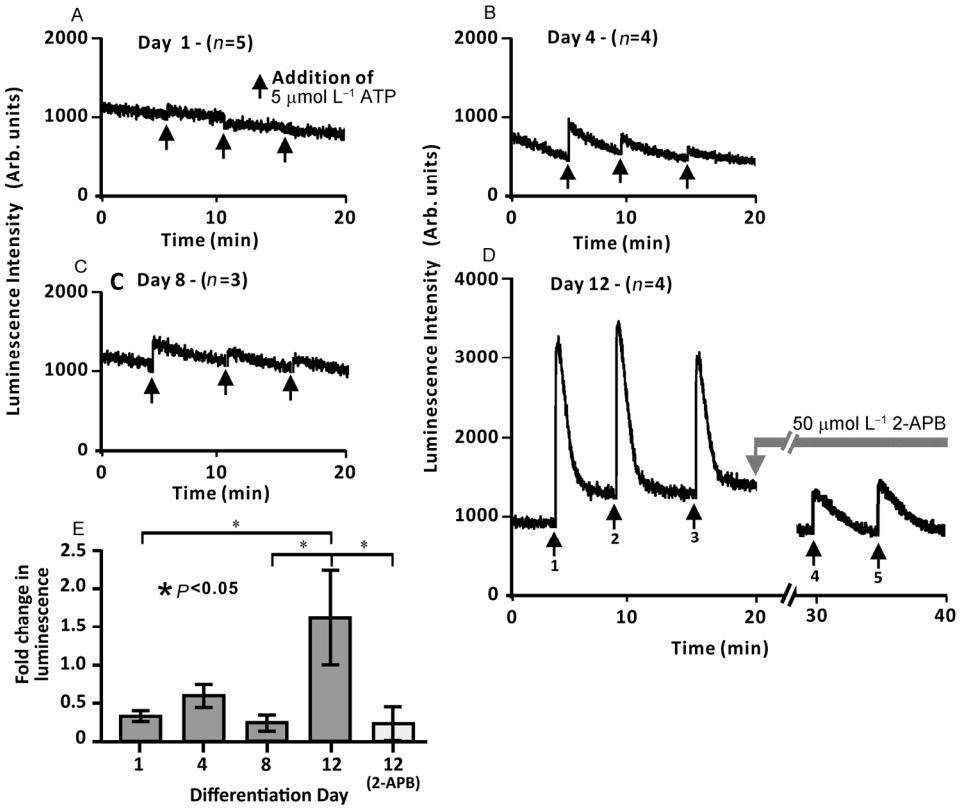

Figure 3 Representative line graphs to show the effect of ATP on the aequorin-generated luminescence in cardiospheres at (A) day 1 (n=5), (B) day 4 (n=4), (C) day 8 (n=3), and (D) day 12 (n=4) of differentiation. Cardiospheres were incubated with *f*-coelenterazine for 45 min, after which they were washed briefly with PBS and then incubated with PBS containing EGTA for the course of the luminescence intensity measurements. At each day of differentiation, 5 μmol L^{-1} ATP was added at three time-points (see black arrows) over a period of ~20 min. On day 12, following the addition of ATP, cells were incubated with 50 μmol L^{-1} 2-APB after which 5 μmol L^{-1} ATP was again added at three time points. E, Bar chart with mean±SEM fold change in luminescence following the first addition of ATP at day 1 to day 12, and following the first addition of ATP after 2-APB treatment at day 12. Asterisks indicate statistically significant results at P<0.05.

luminescence intensity increasing by ~1.0 to 1.3 fold (i.e., from ~523 to ~1,204 cps, and from ~572 to ~1,159 cps after the first and second doses, respectively). After each dose of $CaCl_2$, the luminescence intensity returned to background levels of ~530 and ~542 cps.

Investigating the effect of ATP on the luminescence generated by holo-*f*-aequorin-expressing cardiospheres

Figure 3 shows a series of four line graphs, which illustrate the effect of ATP on the holo-*f*-aequorin-generated bioluminescence in cardiospheres at day 1, 4, 8, and 12 of differentiation.

At differentiation day 1 (Figure 3A), a small increase in the luminescence intensity of ~0.2 fold (i.e., from ~942 to ~1,129 cps) was recorded following the first dose of ATP. However, with the subsequent additions of ATP, no distinct increase in luminescence intensity was recorded. In addition, over the period of 20 min that the experiment was conducted, the overall level of luminescence declined from ~1,080 to ~770 cps.

At differentiation day 4 and day 8 (Figure 3B and C), each of the three applications of ATP stimulated a distinct increase in the luminescence intensity generated by the cardiospheres. In each case, the first dose of ATP produced the strongest increase, although this was more obvious in the day 4 cardiospheres than in the day 8 cells. Hence, at day 4 (Figure 3B), the first dose of ATP stimulated ~1 fold increase in the luminescence intensity (i.e., from ~495 to ~980 cps), whereas the second and third doses only stimulated a ~0.4 fold increase (i.e., from ~554 to ~785 cps, and from ~459 to ~638 cps, respectively). Similarly, at day 8 (Figure 3C), the initial application of ATP stimulated a ~0.3 fold increase in luminescence intensity (i.e., from ~1,085 to ~1,445 cps), whereas the subsequent doses both stimulated a ~0.2 fold increase (i.e., from ~1,093 to ~1,293 cps, and from ~998 to ~1,237 cps, respectively).

At differentiation day 12 (Figure 3D), each of the three applications of ATP generated far more robust increases in luminescence intensity than those observed at the earlier time points. Thus, after the first, second, and third doses of ATP, the luminescence intensity increased by ~2.5, ~1.7 and ~1.4 fold, respectively (i.e., from ~912 to ~3,264 cps, from ~1,264 to ~3,407 cps, and from ~1,234 to ~3,015 cps, respectively). Before the first dose of ATP, the background

level of luminescence was ~910 cps, then after the first dose of ATP, the level of luminescence returned to a background level of ~1,270 cps. After the second and third applications of ATP, the level of luminescence returned to background levels of ~1,280 and ~1,360 cps, respectively. The cardiospheres were then incubated with the IP_3R antagonist, 2-aminoethoxydiphenyl borate (2-APB) for ~15–20 min after which the cells, still bathed in 2-APB, were stimulated with a further two doses of ATP. On addition of 2-APB, the level of luminescence declined gradually from ~1,360 to ~800 cps and then leveled off. The fourth and fifth doses of ATP stimulated small increases in luminescence intensity of just ~0.6 and ~0.75 fold, respectively (i.e., from ~785 to ~1,282 cps, and from ~807 to ~1,423 cps, respectively). Thus, 2-APB treatment inhibited the normal ATP-stimulated increases in luminescence by ~62%. Together, these data suggest that at day 1, the cardiospheres exhibited a minimal response to 5 μmol L^{-1} ATP, but from day 4 to day 12, these cells exhibited an increasing response to such ATP treatment.

Figure 3E shows the mean±SEM fold increase in luminescence at day 1 to day 12 on stimulation with the first dose of ATP, and on day 12 on stimulation with the first dose of ATP following 2-APB treatment. The fold increase at day 12 was significantly greater (at $P<0.05$) than that at day 1 and day 8. In addition, at day 12, the mean±SEM fold increase in luminescence on addition of ATP following 2-APB treatment was significantly lower (at $P<0.05$) than that before treatment.

Investigating the effect of caffeine on the luminescence generated by apo-aequorin-expressing cardiospheres

Figure 4 shows a series of five line graphs; the first four graphs (Figure 4A–D) show the effect of caffeine on the holo-*f*-aequorin-generated bioluminescence in cardiospheres at day 1, 4, 8 and 12 of differentiation, whereas the last graph (Figure 4E) shows a holo-*f*-aequorin "burnout", which was conducted at the end of the day 12 experiment shown in Figure 4D.

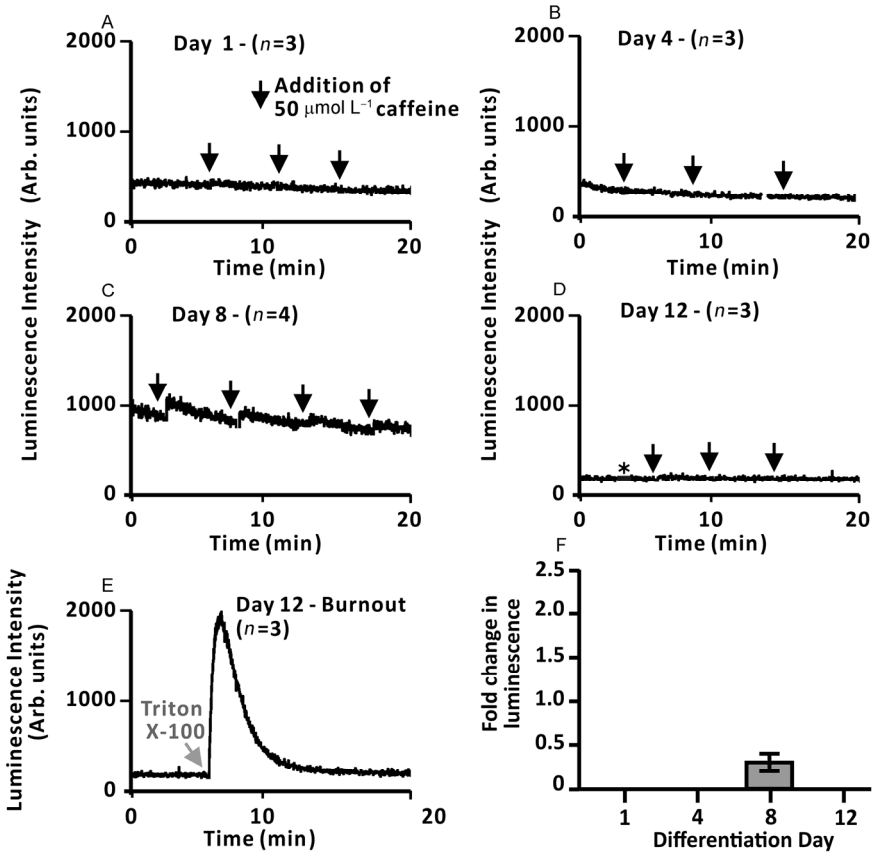

Figure 4 Representative line graphs to show the effect of caffeine on the aequorin-generated luminescence in cardiospheres at (A) day 1 (n=3), (B) day 4 (n=3), (C) day 8 (n=4), and (D) day 12 (n=3) of differentiation. Cardiospheres were incubated with *f*-coelenterazine for 45 min, after which they were washed briefly with PBS and then incubated with PBS containing EGTA for the course of the luminescence intensity measurements. At each day of differentiation, 50 mmol L^{-1} caffeine was added at three time-points (see black arrows) over a period of ~20 min. The asterisk in panel D indicates a brief break (of ~1 min) in the luminescence intensity recording. E, Representative (n=3) line graph to show the effect of adding 5% Triton X-100 on the luminescence intensity at the end of Ca^{2+} recording on Day 12. F, Bar chart with mean±SEM fold change in luminescence following the first addition of caffeine at day 1 to day 12. No statistically significant differences were observed amongst the data.

At differentiation days 1, 4 and 12 (Figure 4A, B and D), the luminescence intensity in the cardiospheres did not change following the three additions of caffeine. At day 8 of differentiation (Figure 4C), however, small increases in luminescence intensity were observed following the addition of caffeine. The change in luminescence intensity was most obvious after the first and second doses of caffeine with an increase of ~0.3 fold for both (i.e., from 841 to 1,128 cps, and from 784 to 985 cps, respectively). The subsequent two doses of caffeine yielded even smaller changes in the luminescence intensity.

Caffeine appeared to exhibit a measurable effect on the luminescence generated by cardiospheres at day 8. However, it did not have an effect at days 1, 4 or 12. ATP treatment (see Figure 3) did indicate that sufficient holo-*f*-aequorin was present in cardiospheres on days 1 and 4, and burnout of the caffeine treated cells on day 12 appeared to confirm this. Figure 4E is a representative example showing the effect of Triton X-100 treatment on the luminescence generated by the day 12 cardiospheres; the luminescence intensity was shown to increase by ~12.5 fold (i.e., from ~146 to ~1,965 cps). Therefore, we suggest that the lack of luminescence observed was a real result and not due to an insufficient amount of unspent holo-*f*-aequorin being present in the cells.

Figure 4F shows the mean±SEM fold increase in luminescence in cardiospheres at day 1 to day 12 on stimulation with the first dose of caffeine. These data show that at day 1, day 4 and day 12 there were no obvious changes in luminescence following the addition of caffeine. There was a slight increase in luminescence at day 8 but this was not significantly different from the data collected on the other days.

DISCUSSION

Preparation of the apo-aequorin-expressing HES2 cells

An apo-aequorin-expressing HES2 hESC line was generated by lentiviral transduction of cells with the ETO-AEQ plasmid. Viral transduction methods have been previously used to genetically express apo-aequorin in the cytosol, or targeted to distinct intracellular organelles, in a variety of cell types, including HeLa cells, adrenal medulla chromaffin cells, HEK293 cells, GH_3 pituitary cells and PC12 cells (Chamero et al., 2002; Missiaen et al., 2004; SantoDomingo et al., 2008). In addition, apo-aequorin has previously been expressed genetically in cardiomyocytes isolated from adult rats (Bell et al., 2006), but this is the first time that the protein has been expressed in hESCs and in hESC-CMs. The HES2 cell line was chosen as it has been previously reported that the vast majority (i.e., over 90%) of cardiomyocytes derived from these cells are ventricular in nature (Mummery et al., 2003; Weng et al., 2014). These cells were transduced with the apo-aequorin plasmid, which also contained the coding sequence for tdTomato. This bright red fluorescent protein was first described over a decade ago (Shaner et al., 2004), and it has been used as a marker to allow the rapid identification and confirmation of successful transduction simply via determining the presence of fluorescence (Salamango et al., 2013). In addition, the EF1α promoter was used, as vectors containing a transgene under the control of this promoter have been demonstrated to efficiently transduce human ESCs (Ma et al., 2003). The visualization of tdTomato fluorescence in our transduced HES2 cells (Figure 1A) indicated that these cells also expressed the apo-aequorin gene. Indeed, the expression of apo-aequorin in this cell line was subsequently confirmed via Western blot (Figure 1B).

The functionality of the apo-aequorin expressed in cardiospheres derived from our transduced HES2 cell line was also tested. Holo-*f*-aequorin was reconstituted in the cardiospheres via incubation for ~45 min with *f*-coelenterazine, after which the level of luminescence generated from these cells in essentially Ca^{2+}-free medium (i.e., PBS containing 5 μmol L^{-1} EGTA) was determined (Figure 2A). No endogenous Ca^{2+} transients could be detected over the 160-min duration of the measurements. However, on the addition of Triton X-100 at the end of these measurements, a considerable amount of aequorin-generated luminescence was released from the cardiospheres (Figure 2B). This indicates that there was sufficient functional holo-*f*-aequorin in the cells to be able to detect changes in intracellular Ca^{2+}. In addition, distinct intracellular Ca^{2+} transients were generated on treatment with KCl and $CaCl_2$ at day 8 and day 18 (Figure 2C and D). It is well known that KCl can induce membrane depolarization in muscle cells, stimulating Ca^{2+} influx via L-type Ca^{2+} channels (Yanagisawa and Okada, 1994; Yu et al., 1995), and the addition of Ca^{2+} can stimulate an increase in intracellular Ca^{2+} via activation of the store-operated Ca^{2+} influx pathway (Apáti et al., 2012). Our results confirmed that the apo-aequorin expressing cells, when bathed in *f*-coelenterazine to reconstitute holo-*f*-aequorin responded as expected when stimulated by treatment with KCl and $CaCl_2$.

It has been previously shown that human ESCs (HUES9 cells) loaded with Fluo-4 exhibit a low level of endogenous intracellular Ca^{2+} signaling in both normal Ca^{2+}-containing and Ca^{2+}-free medium, and that in cardiomyocytes derived from HUES9 cells, Ca^{2+} transients are generated in spontaneously contracting cardiac cells (Apáti et al., 2012, 2013). In addition, spontaneous Ca^{2+} transients were reported in 20-day-old hESC-CMs derived from H7 and HES3 cells (Lee et al., 2011), and in 18–24-day-old HES2-derived CMs on electrical stimulation (Liu et al., 2007). Cardiomyocytes derived from HES2 cells have been reported to begin contracting spontaneously as early as day 8 of differentiation. However, our apo-aequorin expressing HES2-derived cardiomyocytes were not observed to contract even on day 12 of differentiation and no spontaneous Ca^{2+} transients were

observed whether the cardiospheres were kept in Ca^{2+}-containing (data not shown) or Ca^{2+}-free medium (Figure 2A). This indicates a delay in the maturation of these cells, which might be due to the expression of apo-aequorin and/or tdTomato in these cells. In order to investigate the possible role of Ca^{2+} release from intracellular stores at the earliest stages of differentiation (i.e., from day 1 to day 12), experiments were performed in the absence of Ca^{2+} in the incubation medium in order to exclude the possibility of any trans-sarcolemmal Ca^{2+} influx via voltage-gated Ca^{2+} channels, which has previously been reported to occur in these cells (Mummery et al., 2003), or via SOCE (Touchberry et al., 2011) and/or receptor-operated Ca^{2+} entry (Chien et al., 1990; Inoue et al., 2006).

Determination of the presence of functional IP_3Rs and RyRs during the early differentiation of cardiospheres

The ability of the aequorin-expressing HES2-derived CMs to generate Ca^{2+} transients in response to ATP and caffeine was tested to investigate the presence of functional IP_3Rs and RyRs during the earliest stages of differentiation, i.e., days 1 to 12 (Figures 3 and 4). It is well established that in undifferentiated mouse ES cells, Ca^{2+} release from the SR is mediated mainly via IP_3Rs with little-to-no involvement from RyRs (Yanagida et al., 2004; Kapur et al. 2007). In addition, in mouse ESC-derived cardiomyocytes, IP_3Rs and RyRs are both involved in the release of Ca^{2+} from the SR, although the activity of the former decreases and that of the latter increases as differentiation progresses (Fu et al., 2006). In human ESCs, a role for the IP_3R is less well established although it has been reported that when HUES9 cells are treated with ATP, a large increase in intracellular Ca^{2+} is generated (Apáti et al., 2012). We demonstrated that the cardiospheres derived from HES2 cells expressing holo-*f*-aequorin exhibited a relatively low response to 5 μmol L^{-1} ATP on days 1 to 8 but showed an increased response with regards to an elevated level of luminescence intensity at day 12. Use of an IP_3R antagonist, 2-APB (Peppiatt et al., 2003), to inhibit the ATP-generated Ca^{2+} transients confirmed that IP_3Rs are indeed functional in the HES2-derived CMs at these early stages of differentiation (Figure 3). The increase in ATP response between day 8 and day 12 is somewhat comparable to the results described previously, where the expression of IP_3R type 2 increased between day 9 to day 11 in mouse ESC-CMs (Fu et al., 2006). Further work needs to be done to investigate if the IP_3R plays a distinct role in the early differentiation of cardiomyocytes from ESCs or not. However, our results do indicate that IP_3Rs are at least present and functional at these early stages of cardiomyocyte differentiation.

In the apo-aequorin expressing cardiospheres, there were no responses following the addition of 50 mmol L^{-1} caffeine (i.e., a RyR agonist) on days 1, 4 or 12. However, day 8 cardiospheres did show a small Ca^{2+} response to this concentration of caffeine (Figure 4). The lack of response to caffeine on day 12 might have been due to the holo-*f*-aequorin having been inactivated, however, the use of Triton X-100 at the end of each experiment confirmed that sufficient active holo-*f*-aequorin was being expressed by the cells to reveal any distinct signals that were generated. Such an overall lack of response to caffeine has previously been reported in 45 to 60 day old cardiomyocytes derived from H9.2 hESCs (Dolnikov et al., 2005). More recently, caffeine was shown to induce Ca^{2+} release in hES2-derived cardiomyocytes but only in a sub-population (~38%) of these cells when they were at day 18 to 24 (Liu et al., 2007). We therefore suggest that the differences that we observed with respect to the stimulatory effect of caffeine at day 8, but not at day 12, might be likewise due to a small (and potentially variable) fraction of cells that respond to caffeine during early differentiation; or perhaps due to the transient expression of functional RyRs around day 8, which is lost by day 12. Our findings, however, reinforce the previous observation that RyRs are underdeveloped and largely non-functional in the SR of these early differentiated cardiomyocytes (Dolnikov et al., 2005).

Together, our results suggest a possible sequential expression of SR-located Ca^{2+} release channels, where functional IP_3Rs appear before functional RyRs. This is consistent with the expression of these two SR-based receptors during embryogenesis in animal models, where functional IP_3Rs have been shown to be expressed in nearly every cell in mice and zebrafish embryos from the earliest stages of development and expression continues throughout development (Rosemblit et al., 1999; Lee et al., 2003; Leung et al., 2009; Cheung et al., 2011). On the other hand, functional RyRs are not expressed during the early stages of development, but they are expressed later on with the differentiation of excitable cells, including cardiac and skeletal muscle, where the receptors are used for specialized cellular functions such as cell contraction (Rosemblit et al., 1999; Lee et al., 2003; Leung et al., 2009; Cheung et al., 2011). Although we demonstrate that IP_3Rs are functional from day 1 onwards, and that RyRs appear to only be functional at day 8, our current data does not tell us the specific role of either receptor with respect to early differentiation of HES2 ESCs.

In summary, we have demonstrated that HES2 ESCs can be transduced with the apo-aequorin gene and that functional holo-*f*-aequorin can be reconstituted in cardiospheres derived from these cells when they are incubated with *f*-coelenterazine. In addition, at the earliest stages of differentiation, detectable Ca^{2+} signals are generated only in cardiospheres treated with ATP, whereas their response to caffeine is minimal. These data indicate that functional IP_3Rs are expressed in these cells before functional RyRs are. We therefore suggest that the continued development and use of genetically expressed bioluminescent Ca^{2+} reporters such as apo-aequorin might offer an alternative method to explore Ca^{2+} signaling during ESC differentiation, especially when

long-duration Ca^{2+} recordings (i.e., lasting hours to days) are required.

MATERIALS AND METHODS

Generation of the recombinant lentiviral vector carrying the apo-aequorin gene

To generate the ETO-AEQ plasmid (Figure 5A), tdTomato and the apo-aequorin gene were fused via a T2A fusion sequence, and the expression of tdTomato and apo-aequorin were driven by the ubiquitously active EF1α promoter. Recombinant lentiviruses were produced by the co-transfection of HEK293FT cells with lentivirus packaging vectors and the vector of interest gene, as previously described (Zufferey et al., 1997). In brief, 24 h prior to co-transfection, 293FT cells were seeded in poly-D-Lysine-coated T175 flasks at a density of 18×10^6 cells/flask. The supernatant containing the lentiviral particles was harvested at 48 and 72 h post-transfection and stored at −80°C before use.

Generation and maintenance of the stable apo-aequorin-HES2 cell line

The HES2 (NIH code: ES02; ES Cell International Pte., Ltd., Singapore) human embryonic stem cell (hESC) line was maintained in feeder- and serum-free conditions in

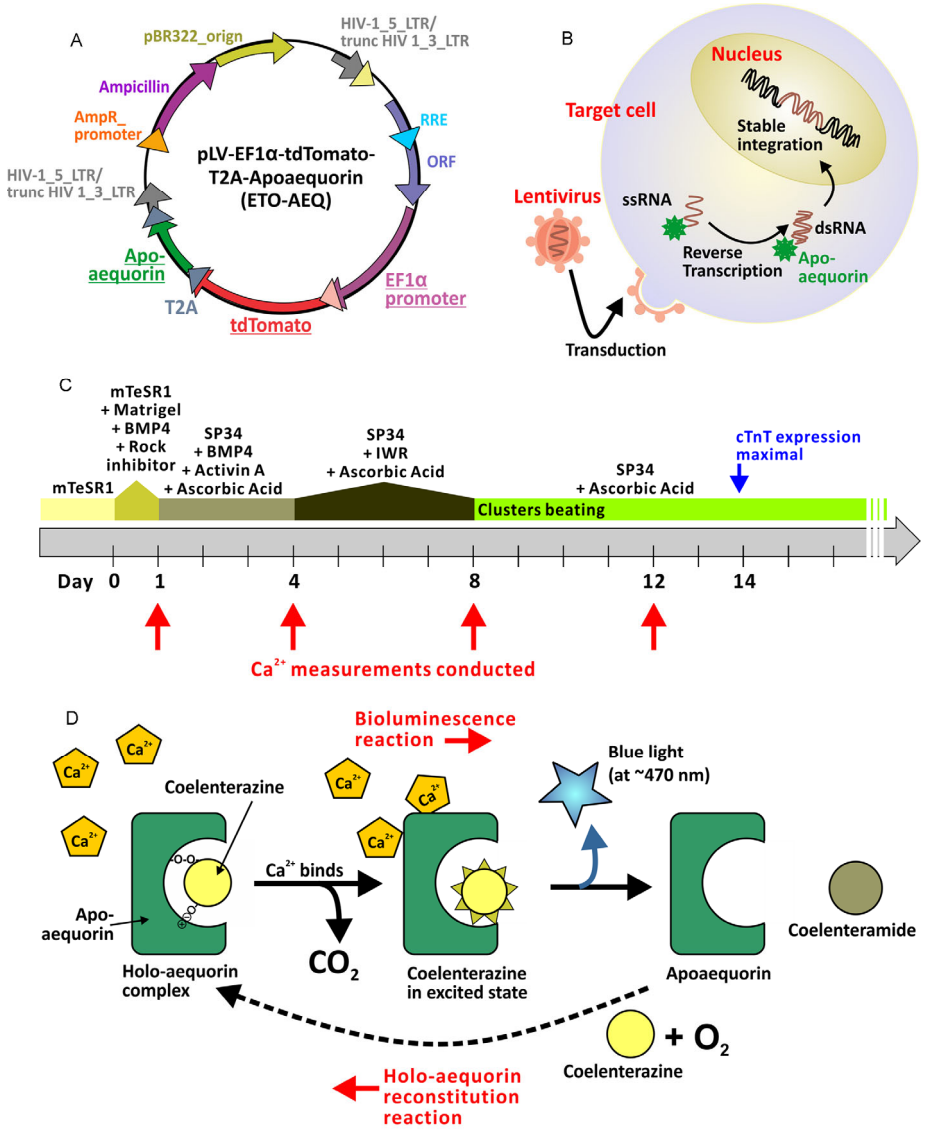

Figure 5 The Ca^{2+} signals generated during the earliest stages of HES2 cell differentiation into cardiomyocytes were observed with the bioluminescent Ca^{2+} reporter, aequorin. A, HES2 cells were transduced with the pLV-EF1α-tdTomato-T2A-Apoaequorin (ETO-AEQ) plasmid. B, Schematic to illustrate the lentivirus transduction process used to generate apo-aequorin-expressing HES2 cells. C, Schematic to show the various components of the culture media used for the first 16 days of differentiation of HES2 cells to cardiomyocytes; the red arrows indicate the days when the Ca^{2+} measurements were made, (modified from Figure 1A of Weng et al., 2014). D, The aequorin bioluminescence reaction, which occurs when Ca^{2+} binds to holo-aequorin and light is generated at ~470 nm.

mTeSR1 (STEMCELL Technologies Inc., Canada) medium on Matrigel- (Discovery Labware, Corning, USA) coated plates at 37°C and 5% CO_2 in a humidified normoxic (i.e., ambient O_2) environment. The tissue culture plates were coated with Matrigel (40 μg mL^{-1}) at 37°C for 30 min just prior to seeding the cells. For stable lentiviral transduction (Figure 5B), the viral supernatant was added to the HES2 cells at a multiplicity of infection of 10, and then they were incubated for 24 h. tdTomato-positive cells were identified by epifluorescence with a Nikon AZ-100 microscope and an AZ-Plan Apo 5x/0.05 NA (both from Nikon Corporation, Japan), with 510–560 nm excitation and 575–590 nm emission. Visualization of tdTomato fluorescence was considered to indicate that the cells also expressed apo-aequorin.

Western blotting

Apo-aequorin expressing HES2 cells were washed with PBS once, and then lysed with ice-cold EBC lysis buffer, consisting of 50 mmol L^{-1} Tris-HCl (pH 8.0), 120 mmol L^{-1} NaCl, 100 mmol L^{-1} NaF, 1 mmol L^{-1} dithiothreitol, 200 μmol L^{-1} Na_3VO_4, 150 nmol L^{-1} phenylmethanesulfonyl fluoride (PMSF), 0.5% sodium deoxycholate, 0.5% Nonidet P-40, 0.1% sodium dodecyl sulfate (SDS), and complete protease inhibitor cocktail (Roche Diagnostics GmbH, Germany), just prior to homogenization. The cell lysate was then homogenized by passing it several times through a 21-gauge needle, after which it was centrifuged at 13,000 r min^{-1} for 10 min at 4°C. The total protein concentration was then measured using the Bradford protein assay (Bio-RAD, USA). The proteins were diluted with SDS sample loading buffer (consisting of 62.5 mmol L^{-1} Tris-HCl, 50% glycerol, 10% SDS, 5% β-mercaptoethanol and 300 μmol L^{-1} bromophenol blue; at pH 6.8) to give a concentration of 30 μg protein per lane, and electrophoresis was conducted with an 8% SDS-polyacrylamide gel for ~1.5 h using a Bio-RAD Mini-Protean Tetra System and Bio-RAD Power Pac Basic. The gel was run for the first 30 min at 80 V, after which the voltage was switched to 120 V for an hour. The SDS-polyacrylamide gel was then transferred to an Immobilon polyvinylidene fluoride (PVDF) membrane (EMD Millipore, Germany), for ~2 h at 100 V, again using the Bio-RAD Tetra and Power Pac. The membrane was blocked with 5% non-fat milk in TBST (20 mmol L^{-1} Tris at pH 7.6, 150 mmol L^{-1} NaCl and 0.1% Tween-20), for ~1 h at room temperature. It was then incubated with primary antibodies against aequorin (ab9096, Abcam, USA; at a dilution of 1∶1,000), and GAPDH (G8795, Sigma-Aldrich Co. LLC., USA; at a dilution of 1∶5,000), at room temperature for ~2 h. After washing with TBST for 3×10 min, the membranes were probed with horse radish peroxidase (HRP)-conjugated anti-rabbit and anti-mouse secondary antibodies, respectively, at room temperature for ~2 h. The membranes were then washed again with TBST for 5×10 min and the protein bands were detected via chemiluminescence using a Luminata Western HRP substrate (EMD Millipore).

Directed cardiac differentiation

hESCs were differentiated into cardiospheres as described previously (Weng et al., 2014; Figure 5C). In brief, large clusters of undifferentiated hESCs were digested into smaller clusters using Accutase (Invitrogen Life Technologies, USA), and then they were seeded onto Matrigel-coated plates at a density of 3×10^5 cells/10 cm^2 in mTeSR1 medium for 4 days until they reached ~80%–90% confluence. This was designated as "day 0". To initiate cardiac differentiation, the hESC clusters were dissociated with Accutase into a single-cell suspension. The cells were then plated into an ultra-low attachment 6-well plate (Corning, USA), and cultured in mTeSR1 medium containing Matrigel (40 μg mL^{-1}), BMP-4 (1 ng mL^{-1}; Invitrogen Life Technologies) and Rho kinase (ROCK) inhibitor (10 μmol L^{-1}; R&D Systems, USA), at 37°C under hypoxic (i.e., 5% O_2) conditions. After 24 h, the culture medium was removed and the cells were washed. They were then incubated with fresh medium, consisting of StemPro34 SFM (Invitrogen Life Technologies) containing ascorbic acid (50 μg mL^{-1}; Sigma-Aldrich), GlutaMAX-1 (2 mmol L^{-1}; Invitrogen Life Technologies), BMP-4 (10 ng mL^{-1}) and human recombinant activin-A (10 ng mL^{-1}; Invitrogen Life Technologies) for 3 days. On day 4, IWR-1, a Wnt inhibitor (5 μmol L^{-1}; Enzo Life Sciences Inc., USA), was added, after which the cardiac mesodermal cells developed into cell clusters (i.e., cardiospheres). On day 8, the cells were transferred to a normoxic (i.e., 21% O_2) environment and maintained in StemPro34 SFM containing 50 μg mL^{-1} ascorbic acid for subsequent culturing.

Temporal Ca^{2+} data acquisition

Cardiospheres were transferred to a glass culture tube and placed in a Titertek-Berthold FB12 Single Tube Luminometer (Berthold Detection Systems GmbH, Germany), linked to a desktop computer, and controlled by the FB12 software. The entire luminometer was warmed using a fan heater (De'Longhi, Italy) to provide temperatures ranging between ~27°C to 32°C in the sample tube. Active holo-aequorin was reconstituted from the apo-aequorin-expressing cardiospheres by incubation with *f*-coelenterazine (NanoLight Technologies, USA) to a final concentration of 5 μmol L^{-1} in StemPro-34 SFM for 45 min. The cardiospheres were then washed once with PBS (137 mmol L^{-1} NaCl, 2.68 mmol L^{-1} KCl, 16 mmol L^{-1} Na_2HPO_4, 5.2 mmol L^{-1} NaH_2PO_4, pH 7.3) for 5 min followed by incubation with 2 mL PBS containing 5 μmol L^{-1} EGTA (Thermo Fisher, USA) for the subsequent holo-*f*-aequorin bioluminescence measurements (Figure 5D). Data collection was paused briefly during the manual addition of *f*-coelenterazine and the agonists used to determine the presence or absence of functional IP_3R and RyR in the cardiospheres. At the end of each data collection experiment, the cardio-

spheres were lysed by the addition of 200 μL PBS containing 5% Triton X-100.

Testing the functionality of reconstituted holo-*f*-aequorin in cardiospheres

In one set of experiments, after holo-*f*-aequorin reconstitution, the background level of luminescence was recorded for a period of 160 min. Data acquisition was then paused briefly while 200 μL PBS containing 5% Triton X-100 was added to the tube containing the cardiospheres and luminescence recording was resumed. The Triton X-100 was used to permeabilize the cardiosphere cells and thus expose any unspent holo-*f*-aequorin to extracellular Ca^{2+}. This confirmed that the low level of aequorin-generated luminescence (and thus the $[Ca^{2+}]$) observed was real and not due to the Ca^{2+} reporter being used up (Leung et al., 2009).

In another series of experiments, after holo-*f*-aequorin reconstitution, the background level of luminescence was recorded for ~1 h, after which data acquisition was paused briefly while 200 μL KCl (Sigma-Aldrich; at 20 mmol L^{-1} in bathing medium) was added to the luminometer tube containing the cardiospheres and recording was resumed. The effect of KCl on the aequorin-generated luminescence was measured for ~5 min, after which in some cases the cardiospheres were treated with a second dose of 20 mmol L^{-1} KCl. Cardiospheres were also treated with 200 μL $CaCl_2$ (Sigma-Aldrich; at 1 mmol L^{-1} in bathing medium), using a similar protocol to that described for the KCl.

Determination of functional IP_3Rs and RyRs in cardiospheres

After holo-*f*-aequorin reconstitution, the background level of luminescence was recorded for ~1 h after which data acquisition was paused briefly. In some experiments, 200 μL ATP (Sigma-Aldrich; at 5 μmol L^{-1} in bathing medium) was added to the tube containing the cardiospheres whereas in other experiments, 200 μL caffeine solution (Sigma-Aldrich; at 50 mmol L^{-1} in bathing medium) was added to the cardiospheres. The effect of ATP or caffeine was measured for a few minutes, after which the cardiospheres were treated with a second dose of either 5 μmol L^{-1} ATP or 50 mmol L^{-1} caffeine, and then with a third dose of ATP or caffeine being added a few minutes later again. The cardiospheres were thus exposed to final [ATP] of 0.45, 0.83 and 1.15 μmol L^{-1} after the first, second and third applications of 5 μmol L^{-1} ATP, respectively, or they were exposed to final [caffeine] of 4.5, 8.3 and 11.5 mmol L^{-1} after the first, second and third applications of 50 mmol L^{-1} caffeine, respectively. As the day 12 cardiospheres generated a robust luminescence response to ATP, they were incubated with 2-APB (Sigma Aldrich) for ~15–20 min, after which the cells were treated with three doses of 5 μmol L^{-1} ATP again. 2-APB was prepared as a stock solution of 30 mmol L^{-1} in dimethyl sulphoxide, after which ~4.3 μL was added to the cardiospheres in the luminometer tube to give a final concentration of 50 μmol L^{-1} 2-APB.

Data analysis

Data were exported to Excel 2013 (Microsoft, USA) for graph plotting, and Minitab 17 (State College, USA) was used to conduct one-way ANOVA to determine statistically significant differences between the data sets.

Compliance and ethics *The author(s) declare that they have no conflict of interest.*

Acknowledgements *We thank Prof. Ronald A. Li of the Stem Cell & Regenerative Medicine Consortium (SCRMC), The Hong Kong University (HKU), Hong Kong for authorizing this project, and the following people from his laboratory for their help: Dr Ken Kwok-Keung Chan for design of the apo-aequorin construct, the preparation of the apo-aequorin-expressing HES2 cells, and student training; and Dr Wendy Keung for maintaining the stable cell line and training HYSC for the ESC and hESC-CM handling. We also thank Ms Ziyang Sun (formerly of the Division of Life Science, the Hong Kong University of Science & Technology; HKUST) for the initial preparation of the apo-aequorin expressing HES2 cell line; Dr Helen Baixia Hao (Division of Life Science, HKUST) for her advice regarding the technical aspects of the Western blotting experiments; and Prof. Kenneth Boheler (SCRMC, HKU, Hong Kong), for his invaluable advice during the course of this project. This work was supported by the Hong Kong Theme-based Research Scheme award (T13-706/11-1), the Hong Kong Research Grants Council (RGC) General Research Fund awards (662113, 16101714, 16100115), the ANR/RGC joint research scheme award (A-HKUST601/13), and the Innovation and Technology Commission (ITCPD/17-9). HYSC was supported by a Hong Kong University Grants Council post-graduate studentship (T13-706/11-11PG).*

Allen, D.G., Gervasio, O.L., Yeung, E.W., and Whitehead, N.P. (2010). Calcium and the damage pathways in muscular dystrophy. Can J Physiol Pharmacol 88, 83–91.

Apáti, A., Pászty, K., Erdei, Z., Szebényi, K., Homolya, L., and Sarkadi, B. (2012). Calcium signaling in pluripotent stem cells. Mol Cell Endocrin 353, 57–67.

Apáti, A., Pászty, K., Hegedüs, L., Kolacsek, O., Orbán, T.I., Erdei, Z., Szebényi, K., Péntek, A., Enyedi, A., and Sarkadi, B. (2013). Characterization of calcium signals in human embryonic stem cells and in their differentiated offspring by a stably integrated calcium indicator protein. Cell Sig 25, 752–759.

Baker, P.F., Hodgkin, A.L., and Ridgway, E.B. (1971). Depolarization and calcium entry in squid giant axons. J Physiol 218, 709–755.

Bell, C.J., Bright, N.A., Rutter, G.A., and Griffiths, E.J. (2006). ATP regulation in adult rat cardiomyocytes: time-resolved decoding of rapid mitochondrial calcium spiking imaged with targeted photoproteins. J Biol Chem 281, 28058–28067.

Berridge, M.J. (1993). Inositol trisphosphate and calcium signaling. Nature 361, 315–325.

Berridge, M.J., Lipp, P., and Bootman, M.D. (2000). The versatility and universality of calcium signaling. Nat Rev Mol Cell Biol 1, 11–21.

Bers, D.M. (2002). Cardiac excitation-contraction coupling. Nature 415, 198–205.

Bers, D.M. (2008). Calcium cycling and signaling in cardiac myocytes. Annu Rev Physiol 70, 23–49.

Bootman, M.D., and Lipp, P. (2001). Calcium signaling and regulation of cell function. eLS doi:10.1038/npg.els.0001265.

Capel, R.A., Bolton, E.L., Lin, W.K., Aston, D., Wang, Y., Liu, W., Wang, X., Burton, R.-A.B., Bloor-Young, D., Shade, K.-T., Ruas, M., Parrington, J., Churchill, G.C., Lei, M., Galione, A., and Terrar, D.A. (2015). Two pore channels (TPC2s) and nicotinic acid adenine dinucle-

otide (NAADP) at lysosomal-sarcoplasmic reticular junctions contribute to acute and chronic β-adrenoceptor signaling in the heart. J Biol Chem 290, 30087–30098.
Chamero, P., Villalobos, C., Alonso, M.T., and García-Sancho, J. (2002). Dampening of cytosolic oscillations on propagation to nucleus. J Biol Chem 277, 50226–50229.
Chang, D.C., and Meng, C. (1995). A localized elevation of cytosolic free calcium is associated with cytokinesis in the zebrafish embryo. J Cell Biol 131, 1539–1545.
Cheung, C.Y., Webb, S.E., Love, D.R., and Miller, A.L. (2011). Visualization, characterization and modulation of calcium signalling during the development of slow muscle cells in intact zebrafish embryos. Int J Dev Biol 55, 153–174.
Chien, W.W., Mohabir, R., and Clusin, W.T. (1990). Effect of thrombin on calcium homeostasis in chick embryonic heart cells: receptor-operated calcium entry with inositol trisphosphate and a pertussis toxin-sensitive G protein as second messangers. J Clin Invest 85, 1436–1443.
Créton, R., Speksnijder, J.E., and Jaffe, L.F. (1998). Patterns of free calcium in zebrafish embryos. J Cell Sci 111, 1613–1622.
Créton, R., Kreiling, J.A., and Jaffe, L.F. (2000). Presence and roles of calcium gradients along the dorsal-ventral axis in *Drosophila* embryos. Dev Biol 217, 375–385.
Dolnikov, K., Shilkrut, M., Zeevi-Levin, N., Gerecht-Nir, S., Itskovitz-Eldor, J., and Binah, O. (2005). Functional properties of human embryonic stem-cell derived cardiomyocytes. Ann N Y Acad Sci 1047, 66–75.
Dolnikov, K., Shilkrut, M., Zeevi-Levin, N., Gerecht-Nir, S., Amit, M., Danon, A., Itskovitz-Eldor, J., and Binah, O. (2006). Functional properties of human embryonic stem-cell derived cardiomyocytes: Intracellular Ca^{2+} handling and the role of sarcoplasmic reticulum in the contraction. Stem Cells 24, 236–245.
Eisen, A., and Reynolds, G.T. (1985). Source and sinks for the calcium released during fertilization of single sea urchin eggs. J Cell Biol 100, 1522–1527.
Fischer, T.H., Maier, L.S., and Sossalla, S. (2013). The ryanodine receptor leak: how a tattered receptor plunges the failing heart into crisis. Heart Fail Rev 18, 475–483.
Fu, J., Yu, H., Wang, R., Liang J., and Yang, H. (2006). Developmental regulation of intracellular calcium transients during cardiomyocyte differentiation of mouse embryonic stem cells. Acta Pharm Sin 27, 901–910.
Galli, G.L.J., Taylor, E.W., and Shiels, H.A. (2006). Calcium influx in turtle ventricular myocytes. Am J Physiol Regul Integr Comp Physiol 6, R1781–R1789.
Gill, C., Mestril, R., and Samali, A. (2002). Losing heart: the role of apoptosis in heart disease—a novel therapeutic target? FASEB J 16, 135–146.
Greenstein, J.L., and Winslow, R.L. (2011). Integrative systems models of cardiac excitation-contraction coupling. Circ Res 108, 70–84.
Griffiths, E.J. (2009). Mitochondrial calcium transport in the heart: physiological and pathological roles. J Mol Cell Cardiol 46, 789–803.
Homa, S.T., Carroll, J., and Swann, K. (1993). Fertilization and early embryology: the role of calcium in mammalian oocyte maturation and egg activation. Hum Reprod 8, 1274–1281.
Hund, T.J., Ziman, A.P., Lederer, W.J., and Mohler, P.J. (2008). The cardiac IP3 receptor: uncovering the role of "the other" calcium release channel. J Mol Cell Cardiol 45, 159–161.
Inoue, R., Jensen, L.J., Shi, J., Morita, H., Nishida, M., Honda, A., and Ito, Y. (2006). Transient receptor potential channels in cardiovascular function and disease. Circ Res 99, 119–131.
Jaffe, L.F. (1999). Organization of early development by calcium patterns. Bioessays 21, 657–667.
Janowski, E., Cleemann, L., Sasse, P., and Morad, M. (2006). Diversity of Ca^{2+} signaling in developing cardiac cells. Ann N Y Acad Sci 1080, 154–164.
Kapur, N., Mignery, G.A., and Banach, K. (2007). Cell cycle-dependent calcium oscillations in mouse embryonic stem cells. Am J Physiol Cell Physiol 292, C1510–C1518.
Knight, M.R., Campbell, A.K., Smith, S.M., and Trewavas, A.J. (1991). Transgenic plant aequorin reports the effects of touch and cold-shock and elicitors on cytoplasmic calcium. Nature 352, 524–526.
Knight, M.R., Smith, S.M., and Trewavas, A.J. (1992). Wind-induced plant motion immediately increases cytosolic calcium. Proc Natl Acad Sci USA 89, 4967–4971.
Knight, M.R., Read, N.D., Campbell, A.K., and Trewavas, A.J. (1993). Imaging calcium dynamics in living plants using semi-synthetic recombinant aequorins. J Cell Biol 121, 83–90.
Kong, C.W., Akar, F.G., and Li, R.A. (2010). Translational potential of human embryonic and induced pluripotent stem cells for myocardial repair: insights from experimental models. Thromb Haemo 104, 30–38.
Konstantinidis K., Whelan, R.S., and Kitsis, R.N. (2012). Mechanisms of cell death in heart disease. Arterioscler Thromb Vasc Biol 32, 1552–1562.
Krane, M. Wernet, O., and Wu, S.M. (2010). Promises and pitfalls in cell replacement therapy for heart failure. Drug Disc Today: Dis Mech 7, e109–e115.
Lee, K.W., Webb, S.E., and Miller, A.L. (2003). Ca^{2+} released via IP_3 receptors is required for furrow deepening during cytokinesis in zebrafish embryos. Int J Dev Biol 47, 411–421.
Lee, Y.K., Ng, K.M., Lai, W.H., Chan, Y.C., Lau, Y.M., Lian, Q., Tse, H.F., and Siu, C.W. (2011). Calcium homeostasis in human induced pluripotent stem cell-derived cardiomyocytes. Stem Cell Rev Rep 7, 976–986.
Lee, Y.K., and Siu, C.W. (2012). Calcium handling in hiPSC-derived cardiomyocytes. Springerbriefs Stem Cells, 61, 1–47.
Leclerc, C., Webb, S.E., Daguzan, C., Moreau, M., and Miller, A.L. (2000). Imaging patterns of calcium transients during neural induction in *Xenopus laevis* embryos. J Cell Sci 113, 3519–3529.
Leung, C.F., Webb, S.E., and Miller, A.L. (1998). Calcium transients accompany ooplasmic segregation in zebrafish embryos. Dev Growth Differ 40, 313–326.
Leung, C.F., Miller, A.L., Korzh, V., Chong, S.-W., Sleptsova-Freidrich, I., and Webb, S.E. (2009). Visualization of stochastic Ca^{2+} signals in the formed somites during the early segmentation period in intact, normally developing zebrafish embryos. Dev Growth Differ 51, 617–637.
Lim, S.Y., Davidson, S.M., Mocanu, M.M., Yellon, D.M., and Smith, C.C. (2007). The cardioprotective effect of necrostatin requires the cyclophilin-D component of the mitochondrial permeability transition pore. Cardiovasc Drugs Ther 21, 467–469.
Linask, K.K., Han, M.D., Artman, M., and Ludwig, C.A. (2001). Sodium-calcium exchanger (NCX-1) and calcium modulation: NCX protein expression patterns and regulation of early heart development. Dev Dyn 221, 249–264.
Liu, W., Yasui, K., Opthof, T., Ishiki, R., Lee, J.K., Kamiya, K., Yokota, M., and Kodama, I. (2002). Developmental changes of Ca^{2+} handling in mouse ventricular cells from early embryo to adulthood. Life Sci 71, 1279–1292.
Liu, J., Fu, J.D., Siu, C.W., and Li, R.A. (2007). Functional sarcoplasmic reticulum for calcium handling of human embryonic stem cell-derived cardiomyocytes: insights for driven maturation. Stem Cells 25, 3038–3044.
Lohmann, C. (2009). Calcium signaling and the development of specific neuronal connections. Prog Brain Res 175, 443–452.
Ma, Y., Ramezani, A., Lewis, R., Hawley, R.G., and Thomson, J.A. (2003). High-level sustained transgene expression in human embryonic stem cells using lentiviral vectors. Stem Cells 21, 111–117.
Ma, L.H., Webb, S.E., Chan, C.M., Zhang, J., and Miller, A.L. (2009). Establishment of a transitory dorsal-biased window of localized Ca^{2+} signaling in the superficial epithelium following the mid-blastula transition in zebrafish embryos. Dev Biol 327, 143–157.
Maddah, M., Heidmann, J.D., Mandegar, M.A., Walker, C.D., Bolouki, S., Conklin, B.R., and Loewke, K.E. (2015). A non-invasive plaform for functional characterization of stem-cell-derived cardiomyocytes with applications in cardiotoxicity testing. Stem Cell Rep 4, 621–631.
Miller, A.L., Karplus, E., and Jaffe, L.F. (1994). Imaging $[Ca^{2+}]_i$ with aequorin using a photon imaging detector. Meth Cell Biol 40, 305–338.
Missiaen, L., Van Acker, K., Van Baelen, K., Raeymaekers, L., Wuytack,

F., Parys, J.B., De Smedt, H., Vanoevelen, J., Dode, L., Rizzuto, R., and Callewaert, G. (2004). Calcium release from the Golgi apparatus and the endoplasmic reticulum in HeLa cells stably expressing target aequorin to these compartments. Cell Calcium 36, 479–487.

Mohamed, T.M., Baudoin-Stanley, F.M., Abou-Leisa, R., Cartwright, E., Neyses, L., and Oceandy, D. (2010). Measurement of plasma membrane calcium-calmodulin-dependent ATPase (PMCA) activity. Methods Mol Biol 637, 333–342.

Mummery, C., Ward-van Oostwaard, D., Doevendans, P., Spijker, R., van den Brink, S., Hassink, R., van der Heyden, M., Opthof, T., Pera, M., Brutel de la Riviere, A., Passier, R., and Tertoolen, L. (2003). Differentiation of human embryonic stem cells to cardiomyocytes: role of coculture with visceral endoderm-like cells. Circ 107, 2733–2740.

Nita, L.I., Hershfinkel, M., and Sekler, I. (2015). Life after birth of the mitochondrial Na^+/Ca^{2+} exchanger, NCLX. Sci China Life Sci 58, 59–65.

Peppiatt, C.M., Collins, T.J., Mackenzie, L., Conway, S.J., Holmes, A.B., Bootman, M.D., Berridge, M.J., Seo, J.T., and Roderick, H.L. (2003). 2-Aminoethoxydiphenyl borate (2-APB) antagonizes inositol 1,4,5-trisphosphate-induced calcium release, inhibits calcium pumps and has a use-dependent and slowly reversible action on store-operated calcium entry channels. Cell Calcium 34, 97–108.

Peterson, O.H., Peterson, C.C.H., and Kasai, H. (1994). Calcium and hormone action. Annu Rev Physiol 56, 297–319.

Poon, E., Kong, C.-W., and Li, R.A. (2011). Human pluripotent stem cell-based approaches for myocardial repair: from the electrophysiological perspective. Mol Pharm 8, 1495–1504.

Porter, G.A. Jr., Makuck, R.F., and Rivkees, S.A. (2003). Intracellular calcium plays an essential role in cardiac development. Dev Dyn 227, 280–290.

Pucéat, M., and Jaconi, M. (2005). Ca^{2+} signaling in cardiogenesis. Cell Calcium 38, 383–389.

Ridgway, E.B., and Ashley, C.C. (1967). Calcium transients in single muscle fibers. Biochem Biophys Res Commun 29, 229–234.

Ridgway, E.B., Gilkey, J.C., and Jaffe, L.F. (1977). Free calcium increases explosively in activating medaka eggs. Proc Natl Acad Sci USA 74, 623–627.

Ringer, S (1883). A further contribution regarding the influence of the different constituents of the blood on the contraction of the heart. J Physiol 4, 29–42.

Rizzuto, R., Simpson, A.W.M., Brini, M., and Pozzan, T. (1992). Rapid changes of mitochondrial Ca^{2+} revealed by specifically targeted recombinant aequorin. Nature 358, 325–327.

Rosemblit, N., Moschella, M.C., Ondriašová, E., Gutstein, D.E., Ondriaš, K., and Marks, A.R. (1999). Intracellular calcium release channel expression during embryogenesis. Dev Biol 206, 163–177.

Rosenberg, S.S., and Spitzer, N.C. (2011). Calcium signaling in neuronal development. Cold Spring Harb Perspec Biol 3, a004259.

Salamango, D.J., Evans, D.A., Baluyot, M.F., Furlong, J.N., and Johnson, M.C. (2013). Recombination can lead to spurious results in retroviral transduction with dually fluorescent reporter genes. J Virol 87, 13900–13903.

SantoDomingo, J., Vay, L., Camacho, M., Hernández-SanMiguel, E., Fonteriz, R.I., Lobatón, C.D., Montero, M., Moreno, A., and Alvarez, J. (2008). Calcium dynamics in bovine adrenal medulla chromaffin cell secretory granules. Eur J Neuro 28, 1265–1274.

Satin, J., Itzhaki, I., Rapoport, S., Schroder, E.A., Izu, L., Arbel, G., Beyar, R., Balke, C.W., Schiller, J., and Gepstein, L. (2008). Calcium handling in human embryonic stem cell-derived cardiomyocytes. Stem Cells 26, 1961–1972.

Sauer, H., Theben, T., Hescheler, J., Lindner, M., Brandt, M.C., and Wartenberg, M. (2001). Characteristics of calcium sparks in cardiomyocytes derived from embryonic stem cells. Am J Physiol Heart Circ Physiol 281, H411–H421.

Schaper, J., Elsasser, A., and Kostin, S. (1999). The role of cell death in heart failure. Circ Res 85, 867–869.

Seidler, T., Hasenfuss, G., and Maier, L.S. (2007). Targeting altered calcium physiology in the heart: translational approaches to excitation, contraction and transcription. Physiol 22, 328–334.

Shaner, N.C., Campbell, R.E., Steinbach, P.A., Giepmans, B.N.G., Palmer, A.E., and Tsien, R.Y. (2004). Improved monomeric red, orange and yellow fluorescent proteins derived from *Discosoma* sp. red fluorescent protein. Nat Biotech 22, 1567–1572.

Shiba, Y., Fernandes, S., Zhu, W.Z., Filice, D., Muskheli, V., Kim, J., Palpant, N.J., Gantz, J., White Moyes, K., Reinecke, H., Van Biber, B., Dardas, T., Mignone, J.L., Izawa, A., Hanna, R., Viswanathan, M., Gold, J.D., Kotlikoff, M.I., Sarvazyan, N., Kay, M.W., Murry, C.E., and Laflamme, M.A. (2012). Human ES-cell-derived cardiomyocytes electrically couple and suppress arrhythmias in injured hearts. Nature 489, 322–325.

Shimomura, O., and Inouye, S. (1996). Titration of recombinant aequorin with calcium chloride. Biochem Biophys Res Communs 221, 77–81.

Silver, R.B. (1996). Calcium, BOBs, QEDs, microdomains and a cellular decision: control of mitotic cell division in sand dollar blastomeres. Cell Calcium 20, 161–179.

Somlo, S., and Erlich, B. (2001). Calcium signaling in polycystic kidney disease. Curr Biol 11, R356–R360.

Splawski, I., Timothy, K.W., Sharpe, L.M., Decher, N., Kumar, P., Bloise, R., Napolitano, C., Schwartz, P.J., Joseph, R.M., Condouris, K., Tager-Flusberg, H., Priori, S.G., Sanguinetti, M.C., and Keating, M.T. (2004). $Ca_v1.2$ calcium channel dysfunction causes a multisystem disorder including arrhythmia and autism. Cell 119, 19–31.

Swann, K., McDougall, A., and Whitaker, M. (1994). Calcium signalling at fertilization. J Mar Biol Assoc UK 74, 3–16.

Szent-Györgyi, A.G. (1975). Calcium regulation of muscle contraction. Biophys J 15, 707–723.

Tian, L., Hires, S.A., Mao, T., Huber, D., Chiappe, M.E., Chalasani, S.H., Petreanu, L., Akerboom, J., McKinney, S.A., Schreiter, E.R., Bargmann, C.I., Jayaraman, V., Svoboda, K., and Looger, L.L. (2009). Imaging neural activity in worms, flies and mice with improved GCaMP calcium indicators. Nat Meth 6, 875–881.

Touchberry, C.D., Elmore, C.J., Nguyen, T.M., Andresen, J.J., Zhao, X., Orange, M., Weisleder, N., Brotto, M., Claycomb, W.C., and Wacker, M.J. (2011). Store-operated calcium entry is present in HL-1 cardiomyocytes and contributes to resting calcium. Biochem Biophys Res Communs 416, 45–50.

Webb, S.E., Lee, K.W., Karplus, E., and Miller, A.L. (1997). Localized calcium transients accompany furrow positioning, propagation, and deepening during the early cleavage period of zebrafish embryos. Dev Biol 192, 78–92.

Webb, S.E., and Miller, A.L. (2003). Calcium signaling during embryonic development. Nat Rev Mol Cell Biol 4, 539–551.

Webb, S.E., Rogers, K.L., Karplus, E., and Miller, A.L. (2010). The use of aequorins to record and visualize Ca^{2+} dynamics: from subcellular microdomains to whole organisms. In M. Whitaker, ed. Methods Cell Biol. (Burlington: Academic Press) pp. 263–300.

Webb, S.E., Fluck, R.A., and Miller, A.L. (2011). Calcium signaling during the early development of medaka and zebrafish. Biochimie 93, 2112–2125.

Weng, Z., Kong, C.W., Ren, L., Karakikes, I., Geng, L., He, J., Chow, M.Z., Mok, C.F., Chan, H.Y.S., Webb, S.E., Keung, W., Chow, H., Miller, A.L., Leung, A.Y., Hajjar, R.J., Li, R.A., and Chan, C.W. (2014). A simple, cost-effective but highly efficient system for deriving ventricular cardiomyocytes from human pluripotent stem cells. Stem Cell Dev 23, 1704–1716.

West, A.E., Chen, W.G., Dalva, M.B., Dolmetsch, R.E., Kornhauser, J.M., Shaywitz, A.J., Takasu, M.A., Tao, X., and Greenberg, M.E. (2001). Calcium regulation of neuronal gene expression. Proc Natl Acad Sci USA 98, 11024–11031.

Whitaker, M. (2006). Calcium at fertilization and in early development. Physiol Rev 86, 25–88.

Woods, N.K., and Padmanabhan, J. (2012). Neuronal calcium signaling and Alzheimer's disease. Adv Exp Med Biol 740, 1193–1217.

Wu, X., Zhang, T., Bossuyt, J., Li, X., McKinsey, T.A., Dedman, J.R., Olson, E.N., Chen, J., Heller Brown, J., and Bers, D.M. (2006). Local $InsP_3$-dependent perinuclear Ca^{2+} signaling in cardiac myocyte excitation-transcription coupling. J Clin Invest 116, 675–682.

Yanagida, E., Shoji, S., Hirayama, Y., Yoshikawa, F., Otsu, K., Uematsu,

H., Hiraoka, M., Furuichi, T., and Kawano, S. (2004). Functional expression of Ca^{2+} signaling pathways in mouse embryonic stem cells. Cell Calcium 36, 135–146.

Yanagisawa, T., and Okada, Y. (1994). KCl depolarization increases Ca^{2+} sensitivity of contractile elements in coronary arterial smooth muscle. Am J Physiol Heart Circ Physiol 267, H614–H621.

Yu, J.Z., Quamme, G.A., and McNeill, J.H. (1995). Altered $[Ca^{2+}]_i$ mobilization in diabetic cardiomyocytes: responses to caffeine, KCl, ouabain and ATP. Diab Res Clin Prac 30, 9–20.

Zhang, P.C., Llach, A., Sheng, X.Y., Hove-Madsen, L., and Tibbets, G.F. (2011). Calcium handling in zebrafish ventricular myocytes. Am J Physiol Integr Comp Physiol 300, R56–R66.

Zhao, Y. T., Valdiva, C.R., Gurrola, G.B., Hernández, J.J., and Valdiva, H.H. (2015). Arrhythmogenic mechanisms in ryanodine receptor channelopathies. Sci China Life Sci 58, 54–58.

Zufferey, R., Nagy, D., Mandel, R.J., Naldini, L. and Trono, D. (1997). Multiply attenuated lentiviral vector achieves efficient gene delivery *in vivo*. Nat Biotech 15, 871–875.